6270 *Macromolecules* **2009**, *42*, 6270–6276
DOI: 10.1021/ma9008498

Macromolecules
ARTICLE

Entangled Polymer Melts: Relation between Plateau Modulus and Stress Autocorrelation Function

Won Bo Lee and Kurt Kremer*

Max Planck Institute for Polymer Research, Ackermannweg 10, 55128 Mainz, Germany

Received April 17, 2009; Revised Manuscript Received July 7, 2009

ABSTRACT: Stress autocorrelation functions (SAF) of entangled polymer melts are calculated by coarse-grained molecular dynamics (MD) simulations. We show that time-averaged stresses reduce the strong noise in SAFs while still capturing most relevant relaxations of the chains. Plateau values of the SAF compare well with plateau values predicted from the entanglement length evaluated via primitive path analysis (PPA) and from experiment (where available). Three types of polymer models are studied: a flexible bead spring model, a semiflexible bead spring model, and a coarse grained bisphenol A-polycarbonate (BPAPC) model. This approach provides a straightforward way to analyze rheological properties of polymer melts on the fly during a simulation.

1. Introduction

Pronounced viscoelasticity is one of the characteristic and most striking properties of polymeric melts. Depending on chemistry, temperature and chain length the time dependent modulus $G(t)$ can either decay exponentially or exhibit a pronounced plateau, once the chains are exceeding a characteristic length, i.e., the entanglement length N_e. This plateau is directly related to the fact that polymeric chains cannot pass through each other and rather have to find other means of relaxation. As a consequence chains eventually are constrained to move within a tube like region around their coarse grained backbone, the so-called primitive path. The plateau modulus, viscosity and entanglement length of such an entangled polymer melt may be calculated from the autocorrelation function of off-diagonal elements of the stress tensor (SAF), since Green−Kubo relations connect these to the SAF. The reptation theory relates the plateau modulus to the entanglement length N_e or entanglement molecular weight M_e,[1−4] respectively. So far however, only a few simulation studies along this line have been performed.[5−11] Due to strong noise, long relaxation times and large spatial scales the evaluation of plateau moduli via the SAF (from MD simulation) still is a challenge from a computational point of view.

Sen et al.[8] calculated the SAF for the standard flexible bead spring polymer (Kremer−Grest, KG) model[12] using averaged stresses (both in time and of all off-diagonal stress elements). This was used to determine an entanglement chain length $N_e = 28$. However, N_e turned out to be about two times smaller than the one evaluated by the primitive path analysis PPA, namely $N_{e,PPA} \simeq 65$.[8,13] The results of the PPA agree well with the results from a direct "measurement" of the restoring force within a deformed simulation box. Recently, the very same model was studied again,[11] now however for systems of more and of longer chains than in ref 8. (up to 100 chains of length $N = 350$ instead of up to 40 chains of $N = 120$), with quite different results. For instance, identifying plateau regions in the SAFs has failed although entanglement effects are clearly observed with increasing chain length. Therefore, a plateau modulus and the corresponding entanglement length have been estimated by an extrapolation procedure and Likhtman et al.,[11] find $N_e = 51.5$. Such a difference might be due to several reasons such as a relatively long entanglement length and information loss of local chain relaxations. The relatively large entanglement length ($N_{e,PPA} \simeq 65$)[13] of the KG model (at a density of $\rho = 0.85\sigma^{-3}$, which is the same in all cases) results in a small plateau value of the SAF, that is difficult to determine with high accuracy and more easily hidden by noise in the system (see section 4).

In addition, coarse-grained MD techniques have also been applied to directly evaluate time dependent elastic modulus of unentangled polymer (short polymer) melts through SAF.[9,10] The data show oscillations caused by stiff bonds at very short time scales (up to $\sim 1\ \tau$) and strong noise with increasing time. In order to reduce the uncertainty at long time scales while maintaining oscillations at short initial time period, the authors of ref 10. suggest a running average method of SAF itself.

As discussed above, a direct evaluation of moduli or viscosities of polymer melts using instantaneous off-diagonal elements of the stress tensor has been tried by various groups,[5−11] however with only limited success. This is not only due to the multiscale aspect (both time and space) but also the characteristic strong noise with an amplitude typically significantly larger than the signal. The plateau values of the SAF usually are so small that the strong noise of the small simulation systems stemming from local chain relaxations and fluctuations can easily hide them, which makes identifying plateau regions really difficult. However, in actual experiments, unlike MD simulations, such a strong noise is not apparent. The reason for that is 2-fold. First experiments deal with macroscopic systems, where thermal fluctuations are properly averaged out. This is not necessarily the case for simulations, since many chains and not just many monomers are needed. Second an experimentally measured stress in a typical rheology experiment is a time-averaged quantity due to limits of the experimental equipment. That is, experimental equipments detect stresses on much coarser level compared with those by (coarse grained) MD simulations ($\sim O(10^{-1})$ ps). Therefore, experimentally measured stresses are inherently preaveraged, where the preaveraging covers the fast local fluctuations. This aspect actually is built in all traditional theories of polymer rheology. In the Rouse model, which is also the basis for the reptation model, inertia terms are ignored because of high friction

*Corresponding author. E-mail: kremer@mpip-mainz.mpg.de.

 Published on Web 07/20/2009

coefficients in polymer melts. That makes the system act *overdamped*. In other words, high frequency modes are already removed. Therefore, both experiments and theory suggest the use of preaveraged stresses, where the high frequency contributions are already integrated out.

In the present paper we make use of exactly this characteristic aspect of theory and measurement and present a direct evaluation of plateau values of SAFs for three different polymer models and show that by such an approach some inherent problems of data analysis can be reduced significantly. Of course, any analysis cannot generate more information than that which is contained in the full simulation trajectory. The optimal analysis of the data thus would be to determine correlation functions between all time steps of the simulation trajectory. This, however even for the modern computer, is impracticable (and would lead to further technical problems). The alternative we suggest here is motivated by the underlying theories and experiments. The three models include the KG model ($N_{e,PPA} \simeq 65$), a semiflexible KG model (KG + angular potentials, $N_{e,PPA} \simeq 28$) and a coarse grained BPAPC model ($N_{e,PPA} \simeq 5.5$).[12−16] The latter one is of special interest, since coarse graining means omitting or averaging out many local details already on the model level. Following the above idea, we systematically study the SAF for time averaged stresses instead of instantaneous stresses.

This paper is arranged in the following way: the simulation models and methods we use are introduced in section 2. There also the use of time-averaged stresses is discussed in more detail. In section 3, results from our simulations for the three different systems are presented and compared to other ways to determine plateau moduli and, where possible, to experiments. In the last section, a short summary and conclusions are provided. In a short appendix, the sensitivity of the results on equilibration issues is discussed.

2. Simulation Model and Methods

The chain models we used are well described in related references[12−16] and system details are only briefly summarized here. For the standard KG model, all beads interact via a purely repulsive Lennard-Jones (LJ) potential (eq 1, WCA potential). Chains are formed by additional attractive interactions, FENE potential (eq 2), which connect nearest neighbors along the backbone. $\mathbf{r}_{ij}$ is the distance vector between i and j beads. σ is the unit of length and ε the unit of energy. The unit of time is

$$\tau = \sqrt{\sigma^2 m/\varepsilon}.$$

The temperature and the mass of each beads are set to 1 ε/k_B and 1 m respectively. To introduce chain stiffness an additional angular potential is added (eq 3), where θ_i is an angle between bonds connecting beads $i-1$, i and i, $i+1$, respectively.[13,14] For the standard KG and the semiflexible model, $k = 30\varepsilon/\sigma^2$ and $R_o = 1.5\,\sigma$ are used. $k_\theta = 1.5\varepsilon$ is applied for the semiflexible KG model.

$$U_{ij}^{LJ}(\mathbf{r}_{ij}) = \begin{cases} 4\varepsilon[(\mathbf{r}_{ij}/\sigma)^{12} - (\mathbf{r}_{ij}/\sigma)^{6}] + \varepsilon & \text{if } \mathbf{r}_{ij} \le 2^{1/6}\sigma \\ 0 & \text{if } \mathbf{r}_{ij} > 2^{1/6}\sigma \end{cases} \quad (1)$$

$$U_{ij}^{FENE}(\mathbf{r}_{ij}) = \begin{cases} -0.5kR_o^2 \ln[1-(\mathbf{r}_{ij}/R_o)^2] & \text{if } \mathbf{r}_{ij} \le R_o \\ \infty & \text{if } \mathbf{r}_{ij} > R_o \end{cases} \quad (2)$$

$$U_{bend}(\theta_i) = k_\theta(1-\cos(\theta_i - \pi)) \quad (3)$$

The BPAPC model is more complex, and the model parameters are determined by the structure based coarse graining method. These parameters are optimized to properly reproduce the structure of a polycarbonate melt. Detailed tests have shown that the speedup compared to all atom simulations is about 10^4 and that both structural and dynamical properties of melts are well reproduced. The model is still close enough to the underlying all atom system, that reintroduction of atomistic details also allows the study of rather local properties by coarse grained simulations. This scale bridging approach is explained in detail in refs 13, 15, and 16. The general parameters of the present MD simulations are summarized in Table 1.

Table 1. MD Simulation Parameters for Each Case[a]

	KG	semiflexible KG	BPAPC
no. of beads per chain (N)	100	100	4/20/60/120
no. of chains (M)	100	100	100/100/100/200
density (ρ)	0.85	0.85	0.85
time step (dt) [τ]	0.01	0.01	0.005
temp [ε/k_B]	1.0	1.0	1.0 ($\cong$570 K)[15]
$N_{e,PPA}$[13,14]	65	28	5.5

[a] All units are LJ units unless indicated.

With these parameters we cover the whole range from very weakly entangled (standard KG model with $N = 100$) to highly entangled (BPAPC model with $N = 60$ and 120) melts. All MD simulations are carried out in the NVT ensemble with a Langevin thermostat ($\Gamma = 0.5\,\tau^{-1}$). Possible effects of the thermostat on SAF for KG model have been studied by comparing results from microcanonical (*NVE*) and canonical (*NVT*) simulations. To avoid any energy drift in the *NVE* simulations a small time step of d$t = 0.001\,\tau$ was used. This then is compared to *NVT* simulations with a Langevin thermostat ($\Gamma = 0.5\tau^{-1}$) and varying time step, as indicated in Figure 1. Considering a relaxation time of the Langevin thermostat ($O(1/\Gamma) \sim 2\,\tau$), we expect the effects to be negligible, as shown in Figure 1a.

After the initial setup[17] the pre-equilibrated chains typically ran for more than three times the disentanglement time (τ_d) of each system. For the long chain BPAPC melts ($N = 60$ and $N = 120$) this was not possible, since their disentanglement times ($\tau_d \sim 1.2 \times 10^7\,\tau$ for $N = 60$ and $\tau_d \sim 1.3 \times 10^8\,\tau$ for $N = 120$) are well beyond the limits of numerical calculations. Therefore, we assume that melts are *equilibrated* after MD runs of about $2 \times 10^6\,\tau$ for $N = 60$ and about $1 \times 10^6\,\tau$ for $N = 120$[16] and control this by comparing the internal structure of long and short chain melts as well as the isotropy of the average radius of gyration tensor over the different samplings.[17]

Stresses are defined via the virial theorem and then preaveraged for further data analysis:

$$\sigma_{ij}(t) = \frac{1}{V}\left(\Sigma_{k=1}^{NM} m_k v_k^{(i)} v_k^{(j)} + \frac{1}{2}\Sigma_{k=1}^{NM}\Sigma_{l=1}^{NM} F_{kl}^{(i)} r_{kl}^{(j)}\right) \quad (4)$$

$$\overline{\sigma}_{ij}(t) = \frac{1}{t_{avg}}\Sigma_{\Delta t=-t_{avg}/2+1}^{t_{avg}/2}\sigma_{ij}(t+\Delta t) \quad (5)$$

Subscripts (k,l) represent each beads and sub(and super)-scripts (i,j) correspond to each tensor and vector components. m_k and $v_k^{(i)}$ are the mass of the kth bead and the ith component of the velocity vector of the kth bead, respectively. The ith component of the force vector acting on a k bead by a l bead is given by $F_{kl}^{(i)}$. On the basis of the definition of σ_{ij}(t) related rheological quantities can be calculated in the usual way. The time dependent modulus $G_{ij}(t)$ is directly related to $SAF_{ij}(t)$ (eq 6) and the shear viscosity can be obtained by integrating $G(t)$ (eq 8). The plateau value of SAF (off-diagonal stress elements) is

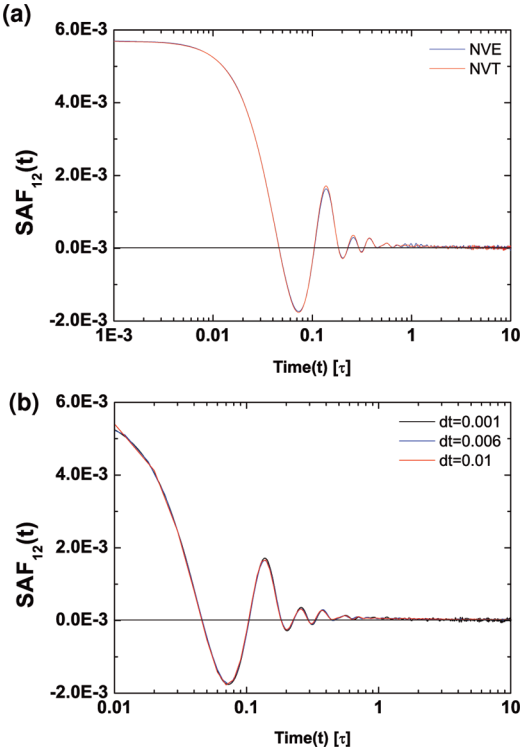

Figure 1. (a) Comparison of the SAF for the standard KG model(N = 100) in the NVE and NVT ensemble wit a small time step of dt = 0.001 τ for both cases. (b) Time step effects on the SAFs of the same model as indicated in the NVT ensemble.

related to the entanglement length (N_e) via linear response (eq 6) and reptation theories (eq 10):[1,2]

$$G_{ij}(t) = \frac{V}{k_B T}\langle \bar{\sigma}_{ij}(t)\bar{\sigma}_{ij}(0)\rangle = \frac{V}{k_B T} SAF_{ij}(t) \tag{6}$$

$$G(t) = \frac{1}{3}(G_{xy}(t)+G_{xz}(t)+G_{yz}(t)) \tag{7}$$

$$\eta = \int_0^\infty G(t)\,\mathrm{d}t \tag{8}$$

$$SAF_{plateau} = \frac{k_B T}{V} G_{plateau} \tag{9}$$

$$G_{plateau} = \frac{4}{5}\frac{\rho k_B T}{N_e} \tag{10}$$

Of course the above ansatz holds only for $t \gg t_{avg}$, the pre averaging time. In order to determine the appropriate t_{avg}, it is assumed, as in theory, that all rheologically relevant contributions to $SAF(t)$ and $SAF_{plateau}$ originate from overdamped motions of the monomers. For this purpose, mean square displacements of beads and velocity autocorrelation functions (VAF) of selected beads are evaluated for the KG model as shown in Figure 2. The crossover from short time ballistic to diffusive motions occurs at about 1 to 10 τ. In addition, the VAF shows a number of oscillations which mainly originate from *longitudinal* relaxations along chain backbones that are faster than *transverse* relaxations.[18,19] Together with slow *transverse* relaxations, VAF shows a negative tail with decaying oscillations.

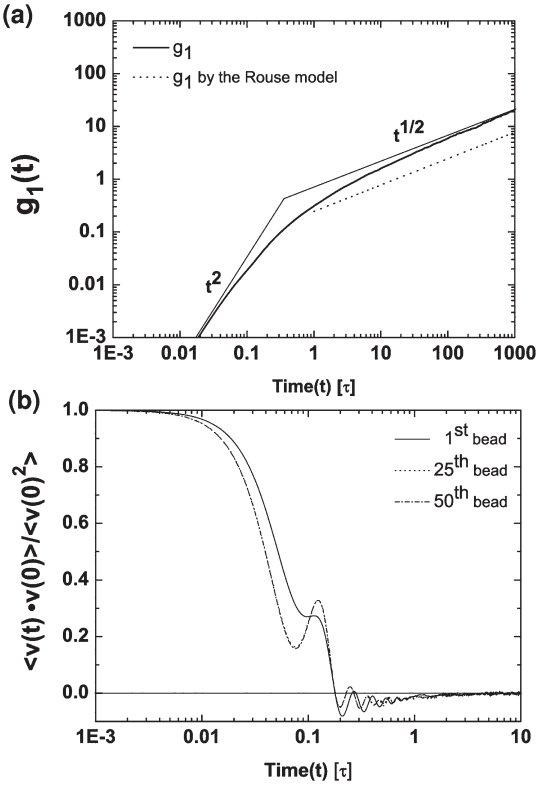

Figure 2. (a) Mean square displacement of beads ($g_1(t) = (1/\mathrm{N})\sum_{i=1}^{N} \langle |r_i(t) - r_i(0)|^2\rangle$ for the KG model (N = 100). The dotted line is drawn based on the Rouse model and the shear viscosity value in Table 2. Since the chain length (N = 100) is not short enough to ensure pure Rouse dynamics (no entanglement effect), the bead friction coefficient is overestimated, which makes the dotted line lower than g_1. (b) Velocity autocorrelation functions of the first, 25th and 50th beads in a chain for KG model (N = 100). Note that the data for bead number 25 and 50 are indistinguishable.

Table 2. Viscosities of the Standard KG Model (N = 100) Evaluated from the Integration of SAF for Various t_{avg} Values

t_{avg} [τ]	0.01	0.1	1	10	100
viscosity [$\varepsilon/\sigma^3 \times \tau$]	133	133	133	133	132

These first results suggest that preaveraging times up to about 100 τ are appropriate. This time is still small compared to typical "machine times" in a rheology experiment.

In addition, we have checked whether the use of preaveraged stresses affect the viscosities. For the standard KG model (N = 100), results are shown in Table 2 as determined by eq 8. As expected, up to t_{avg} = 100 τ, the effect of averaging time to the shear viscosity is negligible.

The value of the shear viscosity in Table 2 is higher than expected from pure Rouse dynamics as indicated in Figure 2a. The chain length (N = 100) used for the KG model is not short enough to completely avoid entanglement effects. Therefore, if an equation for the shear viscosity derived from the Rouse model is used, the bead friction coefficient is overestimated and it predicts lower mean square displacements of beads (the dotted line in Figure 2a) than the real $g_1(t)$. A similar effect can be also found in the value of the diffusion coefficient, which is about 39% underestimated compared with a reference value.[12]

Once an averaging time is applied, instantaneous stresses are changed into time-averaged stresses and SAF's evaluated by them have different characteristics. Therefore, it is crucial to study what are the effects of the averaging time method on SAF. Infinite frequency shear modulus G_∞[20] and SAFs for five different averaging times (t_{avg} = 0.01, 0.1, 1, 10, 100τ) for the semiflexible

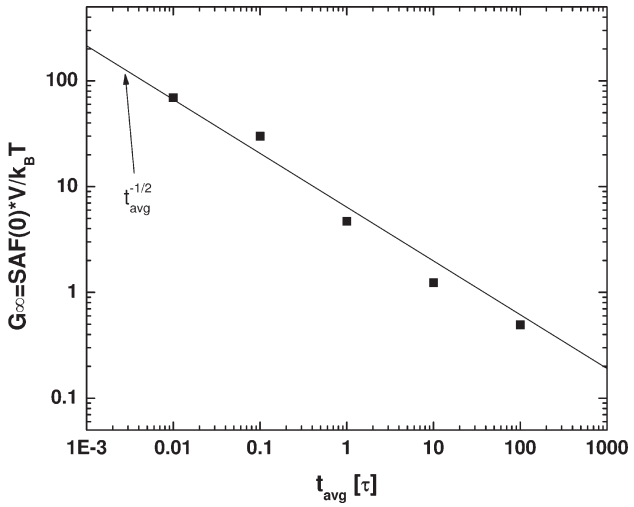

Figure 3. Effects of using time-averaged stress on G_∞ for semiflexible KG model ($N = 100$). For $t_{avg} = 0.01\ \tau$, instantaneous stresses are used since this value is the same as simulation time step.

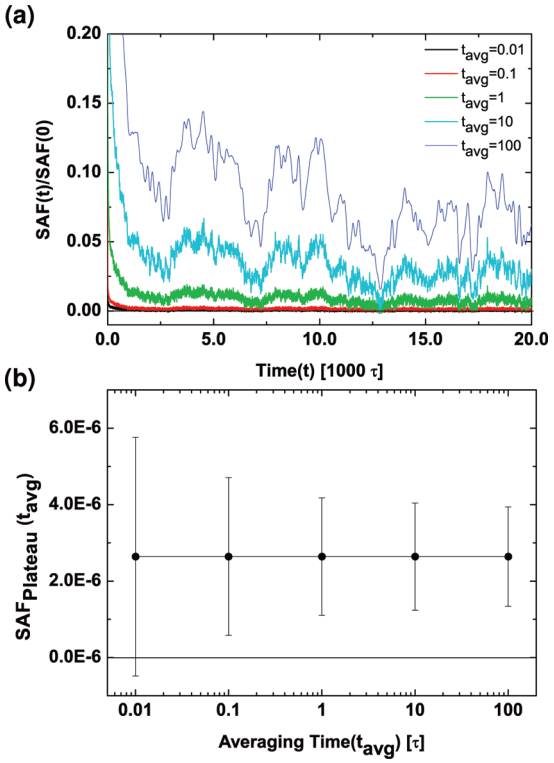

Figure 4. Effects of using time-averaged stress on *SAF* for semiflexible KG model. (a) Normalized SAF (SAF(t)/SAF(0)) at the initial time period. (b) Plateau values of SAF for the semiflexible KG model with $t_{avg} = 0.01, 0.1, 1, 10, 100\ \tau$. In part b, a decay of error bars does not follow $t_{avg}^{-1/2}$ scaling after about $t_{avg} = 1\tau$ since most stochastic contributions are averaged out and local chain relaxations become a major contributor. For $t_{avg} = 0.01\tau$, instantaneous stresses are used since this value is the same as simulation time step (No preaveraging method is applied).

KG model ($N = 100$) are shown in Figure 3 and 4 respectively. As shown in Figure 3, G_∞ decays following $t_{avg}^{-1/2}$ scaling. This is reasonable since G_∞ has only short time limit information originated from mainly stochastic contributions. However, the standard deviations of Figure 4b do not follow $t_{avg}^{-1/2}$ scaling after about $t_{avg} = 1\ \tau$. This is because most stochastic contributions are averaged out and local chain relaxations become a major contributor at long correlation time scale. Overall, for the studied range of averaging times (0.01 to 100τ) only the short time behavior of $SAF(t)$ is affected and the value of $SAF_{plateau}$ does not vary. However the reduction of noise allows us to *see* the plateau modulus. This can be best illustrated by showing the normalized stress autocorrelation function $SAF(t)/SAF(0)$, that demonstrates the signal-to-noise ratio. Without preaveraging the stresses, it would have been almost impossible to detect any plateau value at all, even for the present example of the semiflexible chains of about four N_e.

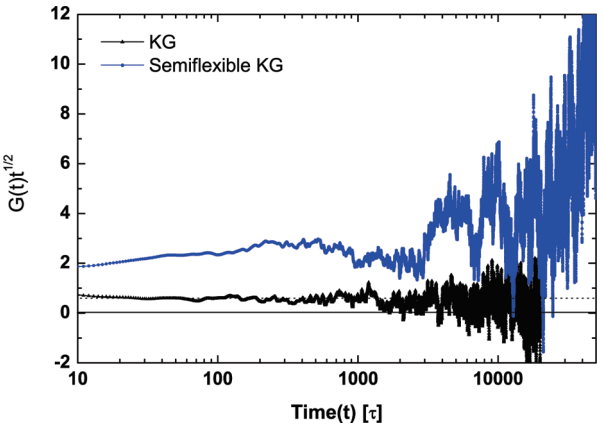

Figure 5. Moduli of KG and semiflexible KG models ($N = 100$ and $M = 100$ for both cases) normalized by Rouse behavior $t^{-1/2}$. A dotted line represents pure Rouse behavior of the KG model[11] (raw data without any further averaging or smoothing).

Based on the above results, we choose $t_{avg} = 10\ \tau$, which corresponds to about 300 ps[21] for the BPAPC systems. During this time span, beads can move about 2σ (see Figure 2), which corresponds to only the immediate surroundings and is significantly smaller than any tube diameter of the present models. This choice of averaging time $t_{avg} = 10\ \tau$ allows us both to minimize the strong noise and to keep almost all chain relaxational information since it is still much smaller than the shortest entanglement time τ_e of all the cases studied here ($\tau_e \sim 600\ \tau$ for the semiflexible KG model).

The computational advantage from the use of preaveraged stresses is practically important since calculating instantaneous SAF requires huge amount of computation time and disk space. For the present study, simulations were especially set up in order to calculate the SAFs and study the effects of the use of preaveraged stresses. Because of that they have been quite time-consuming and required a large storage disk space. When calculating time averaged stresses on the fly, this, however, is just a byproduct of a standard simulation, which can be easily obtained at almost no computational cost.

This preaveraging method is different from the *correlator* algorithm in ref 11 in the sense that the preaveraging method keeps an averaging time constant while the *correlator* algorithm increases its averaging time as correlation time increases.

3. Results and Discussions

The central purpose of our study is to identify plateau regions in SAFs and connect them to corresponding entanglement lengths ($N_{e,SAF}$). Before going into details, it is instructive to see how different and significant entanglement effects are for different models. The present fully flexible and semiflexible bead spring melts are chosen to fit this purpose. We study identical system sizes of $M = 100$ chains of $N = 100$ beads each, however of significantly different entanglement lengths. From a primitive path analysis one obtains $N_{e,PPA} \sim 65$ for the fully flexible model compared to $N_{e,PPA} \sim 28$ for the semiflexible one.[13,14]

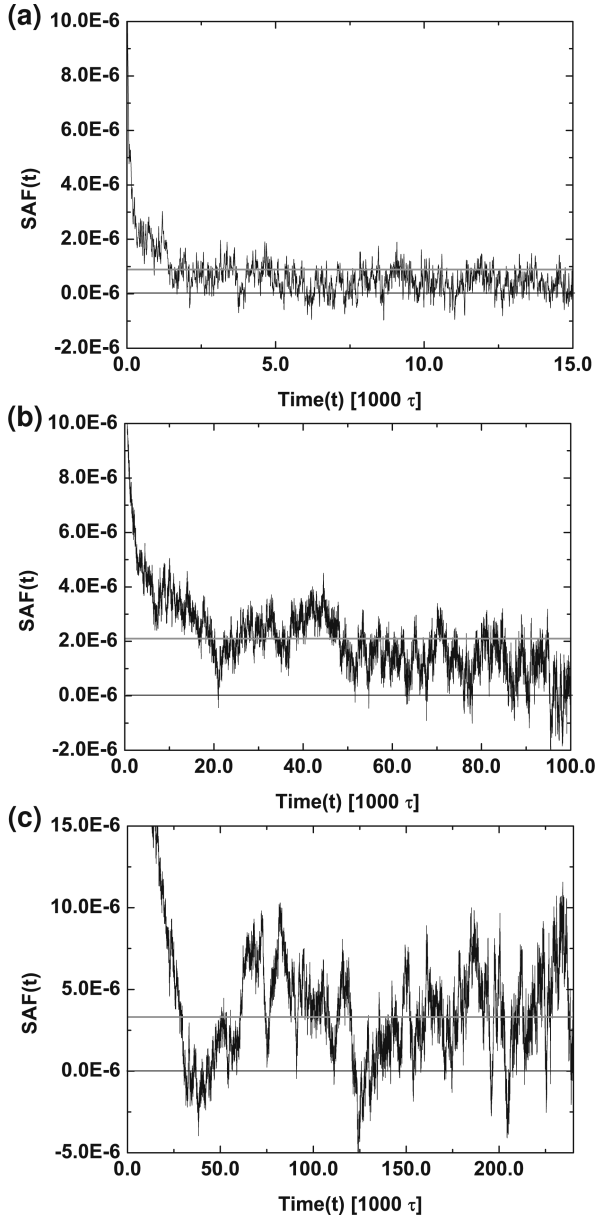

Figure 6. Stress autocorrelation functions for three different systems studied here. Note that the time scales are significantly different is all cases, reflecting the different monomeric friction coefficients. (a) SAF for the KG model ($N=100$); (b) SAF for the semiflexible KG model ($N=100$), averaged over results from three different initial configurations; (c) SAF for BPAPC ($N=20$), averaged over results from three different initial configurations. Green lines represent $SAF_{plateau}$ values calculated from $N_{e,PPA}$[13,14] for very long chains.

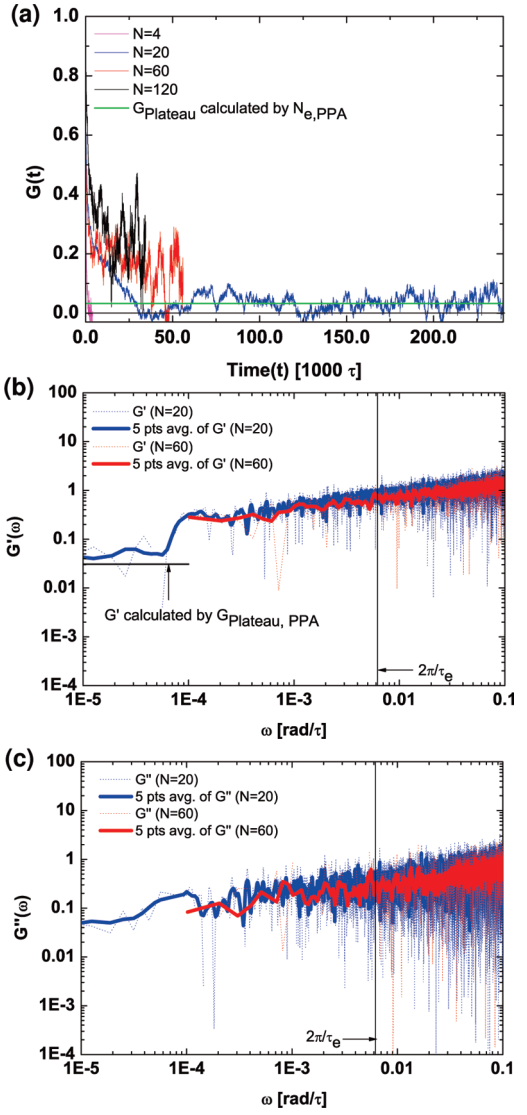

Figure 7. (a) Moduli $G(t)$ for BPAPC ($N=4$, 20, 60, 120). For the $N=20$ case, $G(t)$ is averaged over results from three different initial configurations. The green line represents $G_{plateau}$ calculated by $N_{e,PP}$.[14,13] (b) Storage moduli $G'(\omega)$ for $N=20$ and 60 BPAPC data with $t_{avg}=10\ \tau$. (c) Loss moduli $G''(\omega)$ for $N=20$ and 60 BPAPC data with $t_{avg}=10\ \tau$. In order to reduce fluctuations of G' and G'', averaged lines (5 points average) are also drawn and show a plateau region. Also, at plateau regions, G' (the black line) is calculated based on $N_{e,PPA}$.

These values actually reasonably well agree with the outcome of nonequilibrium simulations. This difference is illustrated in Figure 5, where we plot the moduli of the two models multiplied by $t^{1/2}$. Within the ideal Rouse and reptation picture $G(t)t^{1/2}$ is expected to be constant within the Rouse regime. For times larger than τ_e one observes the plateau in $G(t)$, corresponding to an increase of $G(t)t^{1/2}$. Despite the still significant scatter, it is obvious from Figure 5 that entanglement effects in $G(t)$ and thus in the SAF are observed for the semiflexible melt in contrast to the melt of fully flexible chains.

On the basis of the ratio of N/N_e as determined by the primitive path analysis, melts of semiflexible KG chains of $N=100$ and BPAPC chains of $N=20$ are rather similar. [$N=20$ repeat units consist of 83 beads. However a single repeat unit of BPAPC of four beads is an almost rigid object. These objects are then linked by a very flexible joint at the bead corresponding to the carbonate group of the monomer.] A comparison of all three systems is shown in Figure 6. The strong noise is already reduced by the use of time-averaged stresses. However fluctuations caused by local chain relaxations are still clearly observed. This is not surprising at all taking the small number of chains into account. Especially, the BPAPC case shows relatively strong fluctuations. This most probably comes from the fact that the model has a complicated geometrical structure along the backbone, that includes several angular restrictions. Therefore, local stresses may not relax as smoothly as for the other cases. Additional smoothing might improve the plots somewhat, however a higher precision requires either much bigger samples or much longer runs. These arguments also indicate that proper equilibration is absolutely crucial for the present study, as will be discussed in the appendix. Still the results are quite clear. For comparison the expected asymptotic plateau values for the corresponding fully entangled systems are indicated by green lines. The fully flexible chains are marginally

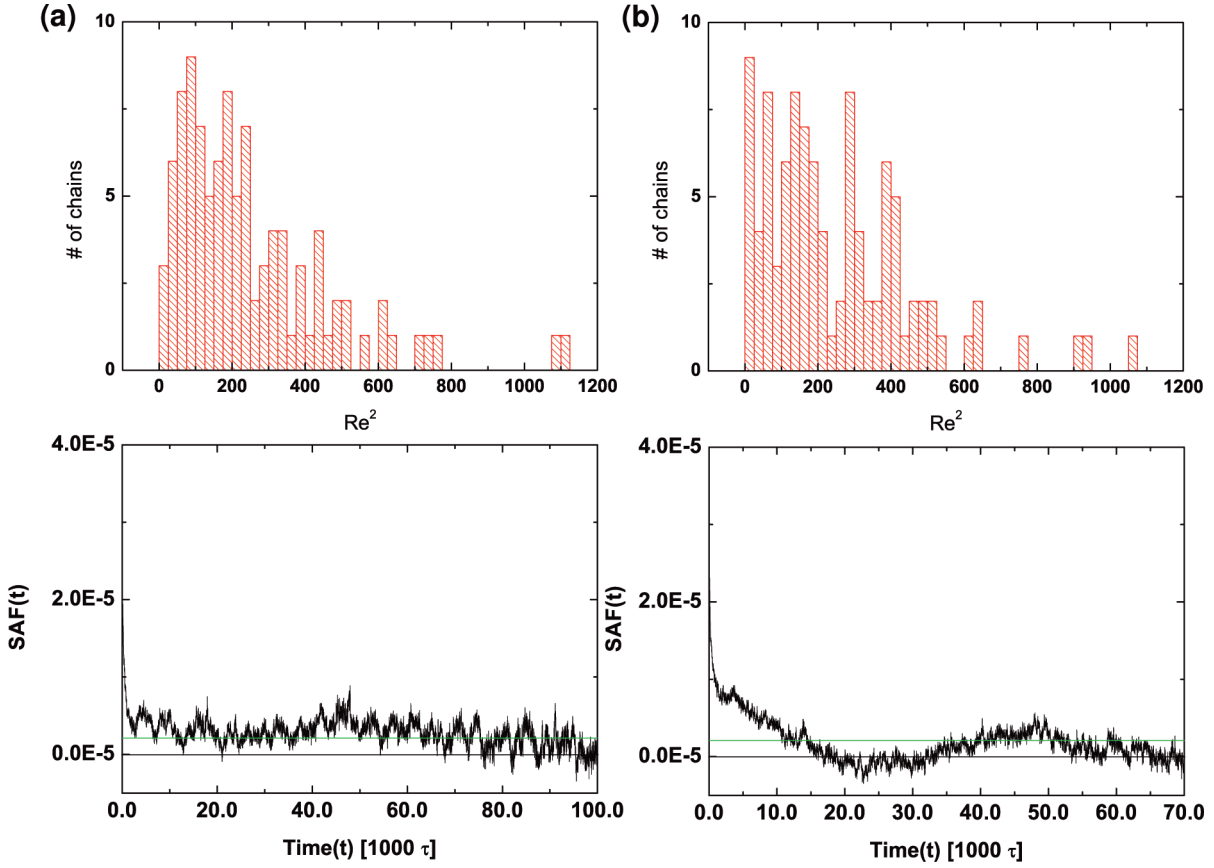

Figure 8. Effects of $R_e^2(N = 100)$ distributions on the SAF. (a) *Proper* R_e^2 distributions for the semiflexible KG model and its resulting SAF. (b) *Improper* R_e^2 distributions for the semiflexible KG model and its resulting SAF. Green lines represent $SAF_{plateau}$ calculated by $N_{e,PPA}$.[13,14]

entangled, if at all. Thus it is not surprising that the observed plateau value is smaller than the asymptotic one. As expected, this reduction is much smaller for the semiflexible chains and not anymore observable (within error bars) for the BPAPC case. In the case of the semiflexible KG model we also nicely observe the disentanglement transition. Taking $\tau_e \approx 600\tau$ we expect a disentanglement time (τ_d) between 40000 and 50000 τ, which again is consistent with Figure 6b. For all three cases studied, plateau regions are clearly identified and in the case of the semiflexible KG model it continues up to about its disentanglement time (τ_d).

For BPAPC equilibrated melts from $N = 4$ up to $M = 200$ chains of $N = 120$ were available from a previous study.[16] This allows us to check the *turn-on* and the persistence of entanglement effects as molecular weight increases, as shown in Figure 7a. Long plateau regions are displayed for $N = 20$ and starting plateau regions for $N = 60$ and $N = 120$. However, the maximal longest time shown here still is much smaller than the terminal disentanglement time for $N = 60$ and $N = 120$. As required for the shortest chains ($N = 4$), $G(t)$ continuously decays and then fluctuates around zero. For $N = 60$ and $N = 120$, the moduli follow a similar path of $G(t)$ for $N = 20$. Storage and loss moduli (G' and G'') of $N = 20$ and 60 cases are generated by the same data set in Figure 7a using discrete Fourier transform[22,23] and provided in Figure 7, parts b and c. In order to avoid end effects, we forced zero after the last data point obtained and drew G' and G'' up to about the maximum correlation time of the actual $G(t)$ data. This, of course, may be done only if $G(t)$ already fluctuates around zero. Values of G' at plateau regions are very close to the value of G' calculated by $N_{e,PPA}$ as shown in Figure 7b, which is also indicated in Figure 7a. In addition, the plots show qualitative agreement with experimental curves. That is, both storage and loss moduli of the $N = 60$ case are almost same as the $N = 20$ case up to available data points. A kink around $\omega = 10^{-4}\tau^{-1}$ for $N = 20$ case in Figure 7b is caused by overdecayed $G(t)$ at about $t = 30000\tau$. Overall, G' is slightly greater than G''. However, a crossover point($\sim 2\pi/\tau_e$) is not clearly visible in the figure.

Table 3. Comparison Entanglement Length (N_e): $N_{e,SAF}$ vs $N_{e,PPA}$[13,14]

	$N_{e,SAF}$	$N_{e,PPA}$
KG	~96	65
semiflexible KG	~31	28
BPAPC	~5.5	5.5

Table 3 summarizes our results for the entanglement molecular weight N_e in comparison to the primitive path analysis (PPA). The agreement is very good. For the fully flexible melt, $N = 100$ corresponds to about $1.5N_e$. These chains are expected to display only a very weak signal of the entanglements if at all. Thus the predicted value of $N_{e,SAF}(N = 100) = 96$ is, as expected, significantly larger than the asymptotic value for that model. For the other two cases however, we have ($N \sim 3.0N_{e,PPA}$) for the semiflexible bead spring chains and almost $N_{max} = 20N_{e,PPA}$ for the longest BPAPC chains. For the latter case the results perfectly agree, while for chains of length $N = 3N_{e,PPA}$ a slightly larger value of N_e is still found. This situation is very similar to what is observed in experiments. Based on our results, we conclude that a minimum chain length to obtain $SAF_{plateau}$ should be greater than $3N_{e,PPA}$ in order to identify plateau regions of entangled polymer melts and obtain a good estimate of the entanglement lengths.

4. Summary and Conclusions

The use of time-averaged stresses for evaluating SAFs in order to identify plateau regions and entanglement lengths has been

applied to three different models for weakly and strongly entangled polymer melts. Preaveraged off-diagonal elements of the stress tensor allow to accurately identify the consequences of structural relaxation. The observed plateau values do not depend on the precise value of the preaveraging time, as long as this time is small enough. As a good estimate of the maximal preaveraging time one can take the crossover time from the ballistic bead motion to the Rouse like $t^{1/2}$ behavior in the mean square displacements of the beads. The values of the resulting plateau modulus compare well with those from the PPA analysis and direct measurements of restoring forces of sheared model systems. To obtain a reliable estimate of the plateau modulus the samples have to be well equilibrated and the chain lengths should be above about $3N_e$. This of course makes it difficult to apply this method for systems with very large N_e, such as semidilute solutions but also polystyrene (PS) melts. For the latter, both experiments and the PPA analysis report entanglement lengths of about 150 repeat units, corresponding to 300 beads in a coarse grained model recently studied by us.[24−26] This leads to very small values for $SAF_{plateau}$, since $SAF_{plateau} \propto N_e^{-1}$ and very good statistics is required to obtain reliable results at all. However keeping these restrictions in mind we have presented a way which allows to directly obtain $G(t)$ and the corresponding plateaus modulus on the fly during a simulation. This also provides an easy path to a direct link between mean square displacements, structural relaxations and rheology, including a very sensitive signal of equilibration. Thus our procedure allows an immediate check of the consistency of models for polymer dynamics and rheology without significant further numerical effort.

Acknowledgment. The authors are grateful to Prof. Dünweg, V. Harmandaris, J. Lee, C. Peter, and B. Hess for their useful discussions and help. This work was supported in part by the Alexander von Humboldt Foundation and the MMM initiative of the Max Planck Society.

Appendix

Due to the typically small values of $SAF_{plateau}$, the number of chains(M) has to be large enough to ensure *proper* chain statistics. Alternatively one would need many runs, which significantly exceed the largest relaxation time in the system. With a limited system size and simulation time, which is typical in MD simulations, *improper* statistics might provide *unrealistic* long-ranged correlations to SAF. In other words, SAF is very sensitive than other properties and can be used as one of criteria for equilibration. How sensitive our analysis is with respect to chain equilibration is shown here. For instance, for the case of the semiflexible KG model, Figure 8 shows the results of two different melts each of M = 100 chains. In both cases the average squared radius of gyration is within the expected error bars (R_g = 6.30 ± 1.4 for case a and R_g = 6.40 ± 1.6 for case b), while the distribution is different. Parts a and b of Figure 8 are for equilibrated melts that are prepared after simulations taking more than triple of its disengagement time ($\tau_d \sim 10^5\,\tau$). Figure 8 shows the instantaneous distribution of the squared end to end distances at the starting point of the analysis and the resulting SAFs. However, the R_e^2 distribution for the second case (Figure 8b) does not look like the characteristic Gaussian one finds by a long time averaging, especially in the small R_e^2 region, which causes long-ranged correlations in its SAF. The small shift in R_e^2 distributions causes a serious effect in the SAF, since the preaveraged SAF only picks up structural relaxations on a scale above the bond length and is thus very susceptible to weak deviations from equilibrium distributions. In order to understand the characteristic frequencies of variations, a Fourier mode analysis of its SAF reveals several peaks at low frequencies-($2\pi\omega = 0.1\times10^{-3}\,\tau^{-1}$) that are close to a time interval between its entanglement and Rouse time. Thus our preaveraging procedure also very sensitively signals equilibration problems, which otherwise might be missed. This also suggests some interesting applications for nonequilibrium studies.

References and Notes

(1) de Gennes, P. *Scaling Concept in Polymer Physics*; Cornell University Press: Ithaca, NY, 1979.
(2) Doi, M.; Edwards, S. F. *The Theory of Polymer Dynamics*; Oxford University Press: Oxford, U.K., 1986.
(3) Likhtman, A. E.; McLeish, T. C. B. *Macromolecules* **2002**, *35*, 6332–6343.
(4) McLeish, T. C. B. *Adv. Phys.* **2002**, *51*, 1379–1527.
(5) Mondello, M.; Grest, G. S. *J. Chem. Phys.* **1997**, *106*, 9327–9336.
(6) Harmandaris, V. A.; Mavrantzas, V. G.; Theodorou, D. N. *Macromolecules* **2000**, *33*, 8062–8076.
(7) Padding, J. T.; Briels, W. J. *J. Chem. Phys.* **2004**, *120*, 2296–3002.
(8) Sen, S.; Kumar, S. K.; Keblinski, P. *Macromolecules* **2005**, *38*, 650–653.
(9) Vladkov, M.; Barrat, J.-L. *Macromol. Theory Simul.* **2006**, *15*, 252–262.
(10) Sen, S.; Kumar, S. K.; Keblinski, P. *J. Chem. Phys.* **2006**, *124*, 144909.
(11) Likhtman, A. E.; Sukumaran, S. K.; Ramirez, J. *Macromolecules* **2007**, *40*, 6748–6757.
(12) Kremer, K.; Grest, G. S. *J. Chem. Phys.* **1990**, *92*, 5057–5086.
(13) Everaers, R.; Sukumaran, S. K.; Grest, G. S.; Svaneborg, C.; Sivasubramanian, A.; Kremer, K. *Science* **2004**, *303*, 823–826.
(14) Auhl, R.; Everaers, R.; Grest, G. S.; Kremer, K.; Plimpton, S. J. *J. Chem. Phys.* **2003**, *119*, 12718–12728.
(15) Abrams, C. F.; Kremer, K. *Macromolecules* **2003**, *36*, 260–267.
(16) León, S.; van der Vegt, N.; Site, L. D.; Kremer, K. *Macromolecules* **2005**, *38*, 8078–8092.
(17) Auhl, R.; Everaers, R.; Grest, G. S.; Kremer, K.; Plimpton, S. J. *J. Chem. Phys.* **2003**, *119*, 12718–12728.
(18) Kopf, A.; Dünweg, B.; Paul, W. *J. Chem. Phys.* **1997**, *107*, 6945–6955.
(19) Balucani, U.; Brodholt, J. P.; Vallauri, R. *J. Phys.: Condens. Matter* **1996**, *8*, 6139–6144.
(20) Zwanzig, R.; Mountain, R. D. *J. Chem. Phys.* **1965**, *43*, 4464–4471.
(21) Hess, B.; León, S.; van der Vegt, N.; Kremer, K. *Soft Matter* **2006**, *2*, 409–414.
(22) Arridge, R. G. C. *J. Phys. D: Appl. Phys.* **1984**, *17*, 1101–1105.
(23) Arridge, R. G. C.; Barham, P. J. *J. Phys. D: Appl. Phys.* **1986**, *19*, L89–L96.
(24) Harmandaris, V. A.; Adhikari, N. P.; van der Vegt, N. F. A.; Kremer, K. *Macromolecules* **2006**, *39*, 6708–6719.
(25) Harmandaris, V. A.; Adhikari, N. P.; van der Vegt, N. F. A.; Kremer, K.; Mann, B. A.; Voelkel, R.; Weiss, H.; Liew, C. *Macromolecules* **2007**, *40*, 7026–7035.
(26) Harmandaris, V. A.; Kremer, K. *Macromolecules* **2009**, *42*, 791–802.